

Structural Characterization of Interactions between the Double-Stranded RNA-Binding Zinc Finger Protein JAZ and Nucleic Acids

Russell G. Burge, Maria A. Martinez-Yamout, H. Jane Dyson and Peter E. Wright

Supplementary Material

Supplementary Figure Captions

Figure S1. Representative EMSA gels showing binding of JAZ zinc finger constructs (shown in Figure 1B) to various nucleic acid constructs (shown in Figure S2 and S3). In each panel A-D and F-G, the first lane has free RNA, with a protein concentration of 4 nM in the second lane. The protein concentration in subsequent lanes was doubled to give a final concentration of ZF34 of 1 μ M in the tenth lane. A. multipartite binding of ZF34 to T52 RNA. B. binding of ZF34 to T57B. C. binding of ZF34 to Duplex 1. D. addition of ZF34 to single-stranded RNA shows no interaction. E. competition of binding of ZF34 to T57A RNA by the addition of cold T57 RNA. F. competition assay showing that ZF34 binds preferentially to T57A RNA over tRNA. Left panel shows ZF34 binding to T57A in the absence of tRNA, right panel shows the same experiment in the presence of excess cold tRNA. G. addition of ZF4 to T57 RNA shows no interaction.

Figure S2. Diagrammatic summary of the RNA constructs that showed relatively strong binding (according to C_{50} values) in EMSA experiments. RNA secondary structure was derived using MFold.¹

Figure S3. Diagrammatic summary of the RNA constructs that showed low or weak binding (according to C_{50} values) in EMSA experiments. RNA secondary structure was derived using MFold.¹

Figure S4. A. Superposition of a part of the 600 MHz HSQC spectrum of ZF3 (50 μ M) in the presence of 100 μ M VAImin (red) and VAIminMut (blue). B. 500 MHz HSQC titration of ZF3 (110 μ M) with a duplex DNA of sequence corresponding to VAImin (final concentration 180 μ M). (Inset) Imino resonances of the DNA duplex, which are unchanged during the titration.

Figure S5. ITC titrations of JAZ ZF23 with (upper) VAImin RNA and VAIminMut RNA (lower).

Figure S6. HSQC spectra of single-finger constructs of JAZ showing assignments. A. ZF1. B. ZF2. C. ZF3. D. ZF4.

Figure S7. 600 MHz 2D ^1H - ^{15}N HMQC spectrum showing connectivities between the side chain ring nuclei of histidine residues. The zinc-coordinating residues H203 ($\text{N}^{\epsilon 2}$) and H209 ($\text{N}^{\delta 1}$) are indicated in green and red respectively.

Figure S8. Overlays of the lowest-energy structure of JAZ ZF3 with A. the lowest-energy structure of the ZFa ZF1 ensemble² and B. the IPTase zinc finger structure derived from the tRNA structure.³ In part A, JAZ ZF3 is colored pink and ZFa ZF1 is colored blue, with an additional N-terminal helix that is not present in the JAZ fingers shown in gray. In part B, JAZ ZF3 is colored blue and the IPTase zinc finger red.

Reference

1. Zuker, M. (2003) Mfold web server for nucleic acid folding and hybridization prediction. *Nucleic Acids Res.* **31**, 3406-3415.
2. Möller, H.M., Martinez-Yamout, M.A., Dyson, H.J., and Wright, P.E. (2005) Solution structure of the N-terminal zinc fingers of the *Xenopus laevis* double-stranded RNA-binding protein ZFa. *J. Mol. Biol.* **351**, 718-730.
3. Zhou, C. and Huang, R.H. (2008) Crystallographic snapshots of eukaryotic dimethylallyltransferase acting on tRNA: Insight into tRNA recognition and reaction mechanism. *Proc. Natl. Acad. Sci. USA* **105**, 16142-16147.

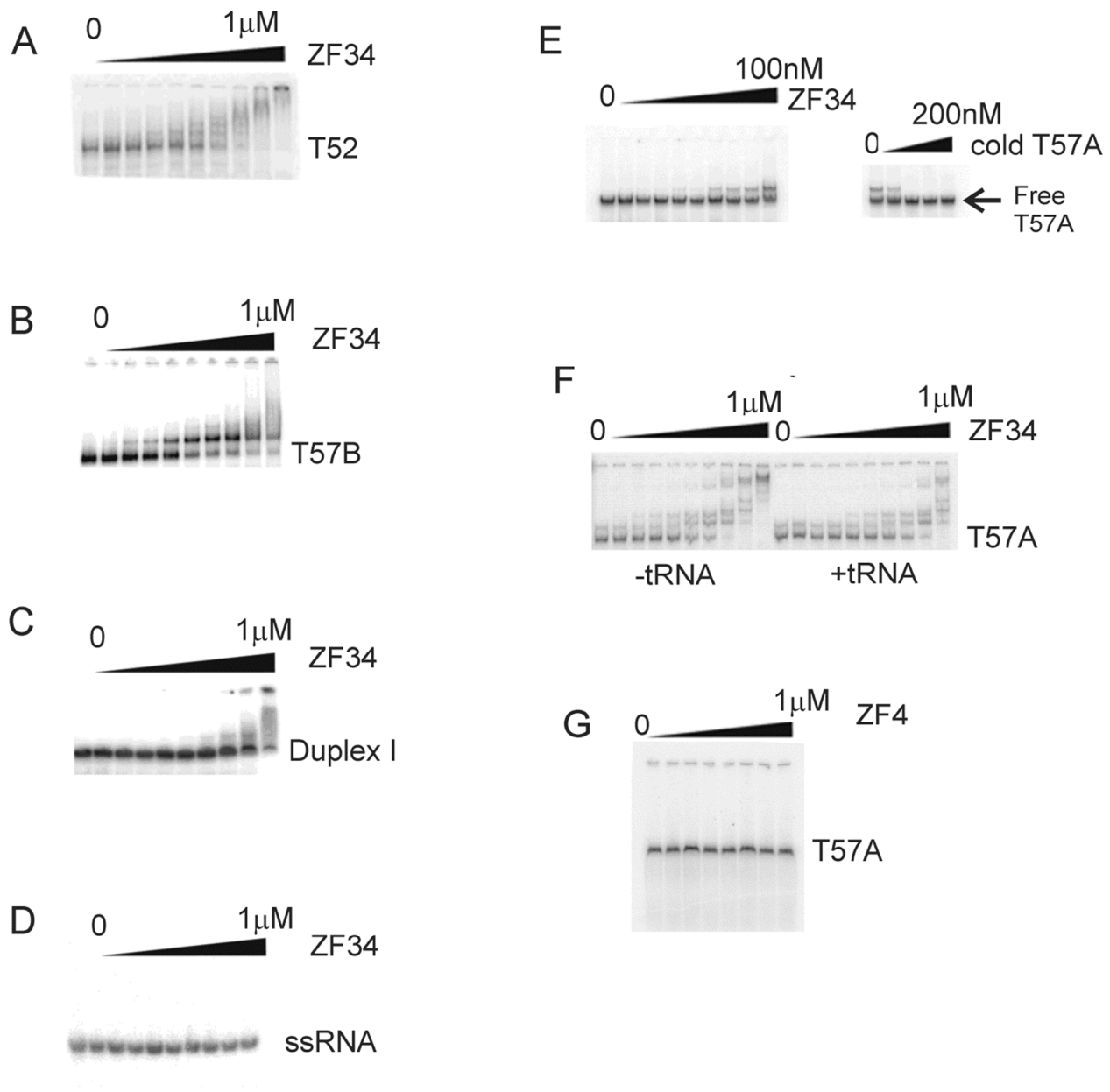


Figure S1

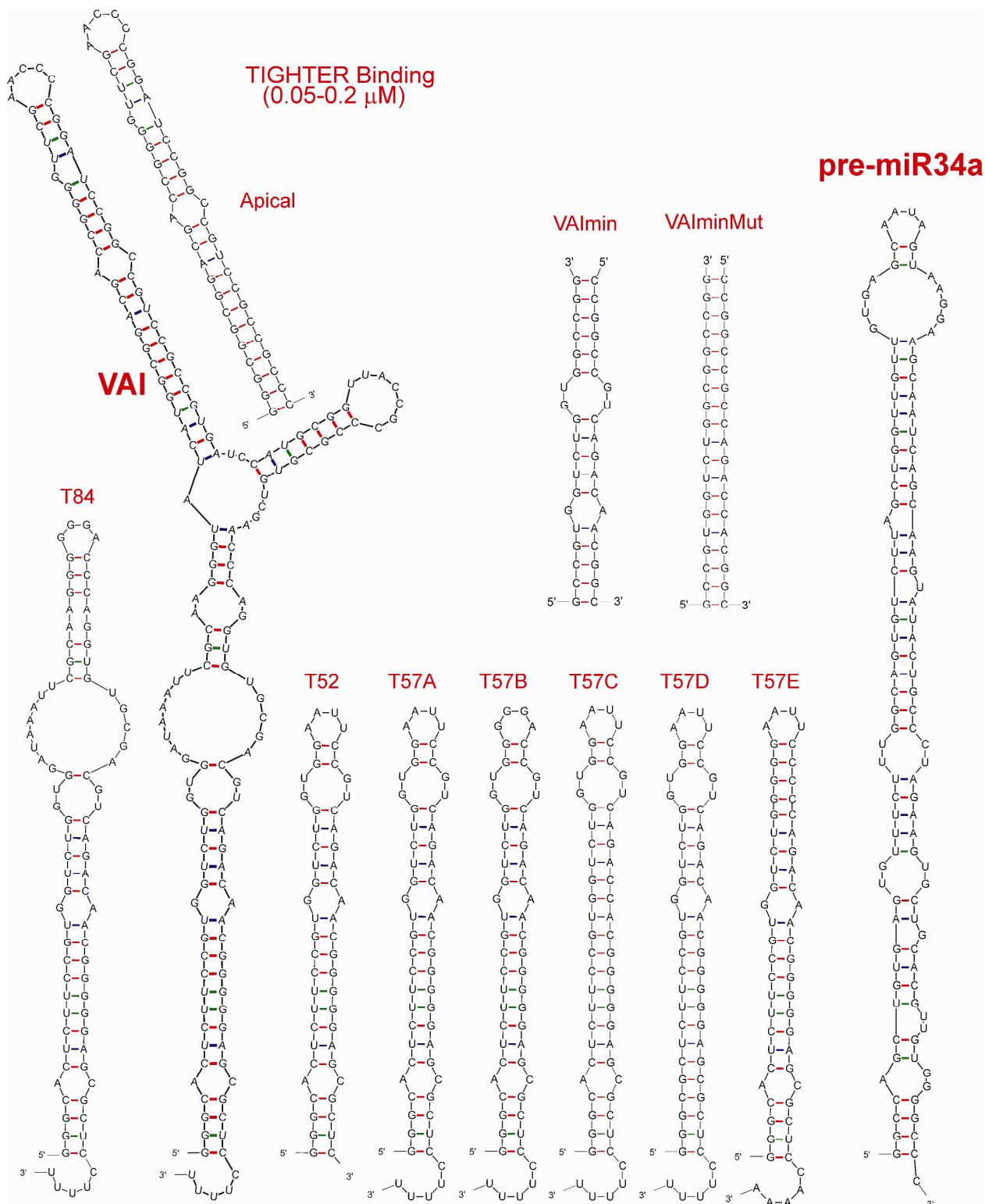


Figure S2

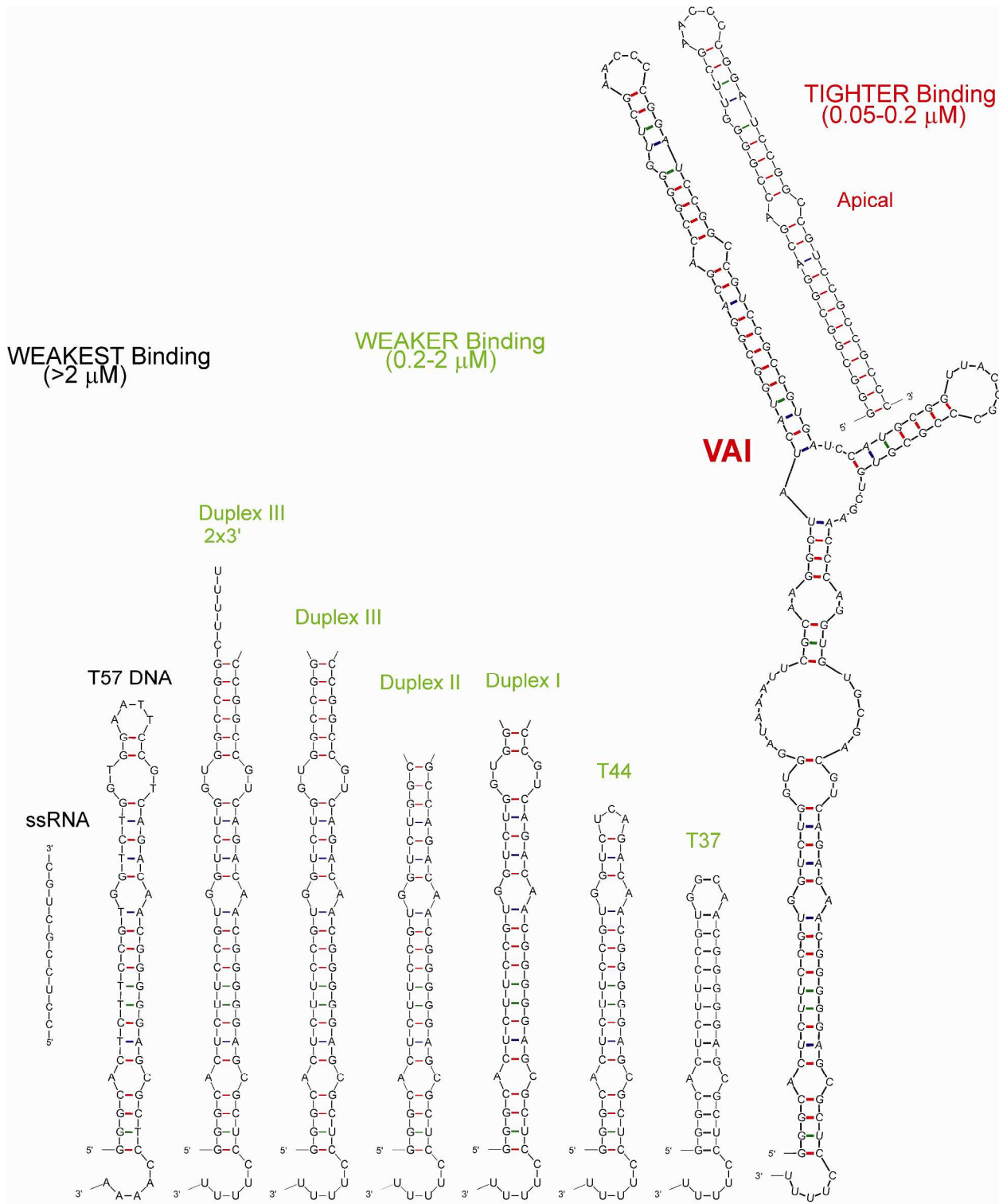


Figure S3

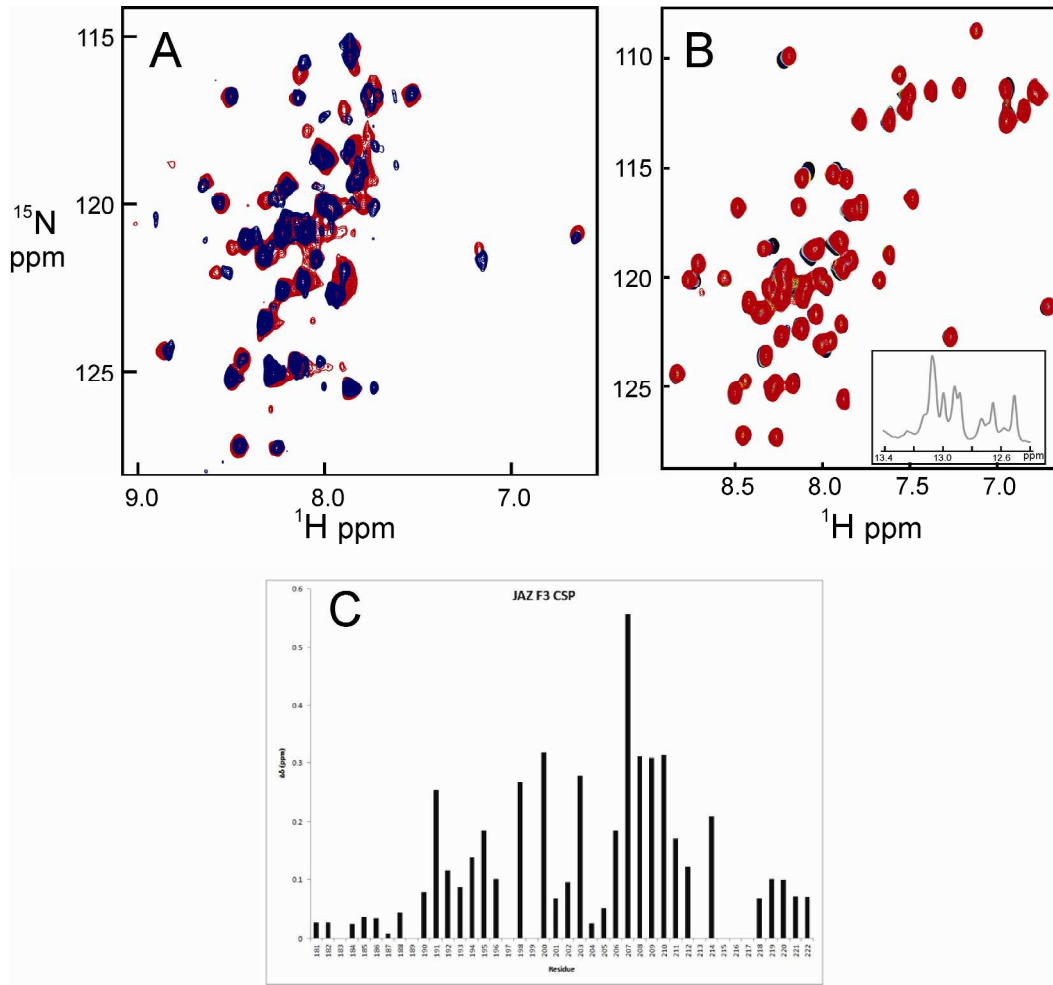
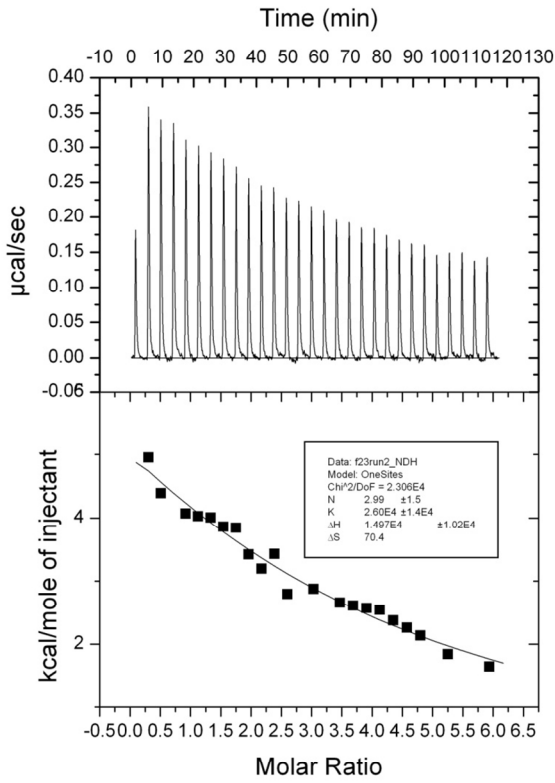
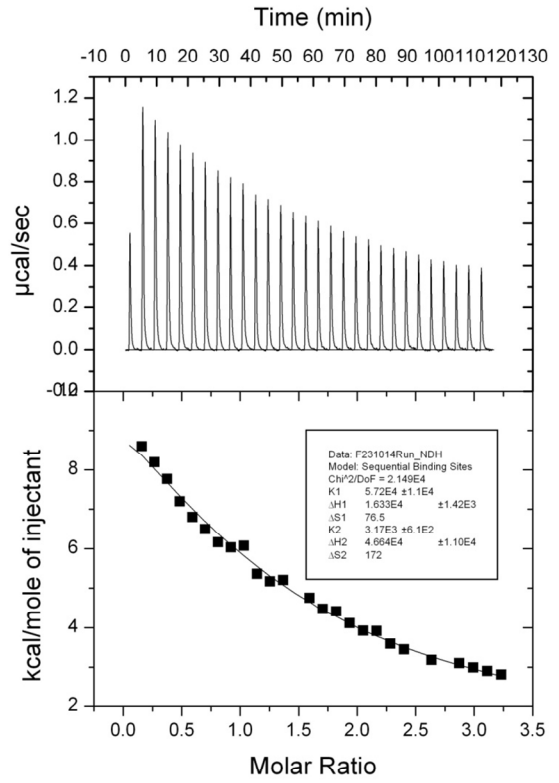


Figure S4



JAZ ZF23 VAlmin RNA



JAZ ZF23 30bps dsRNA

Figure S5

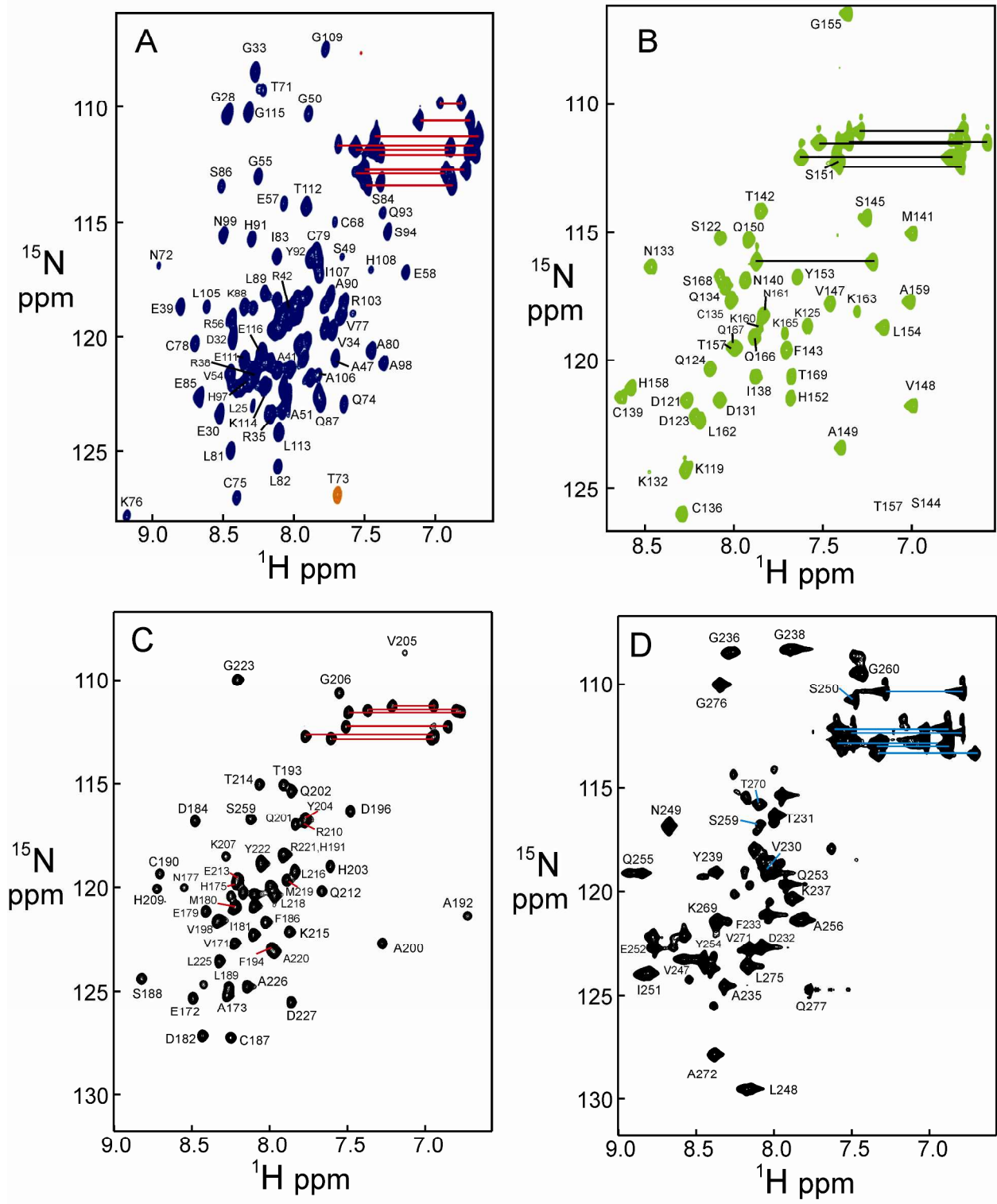


Figure S6

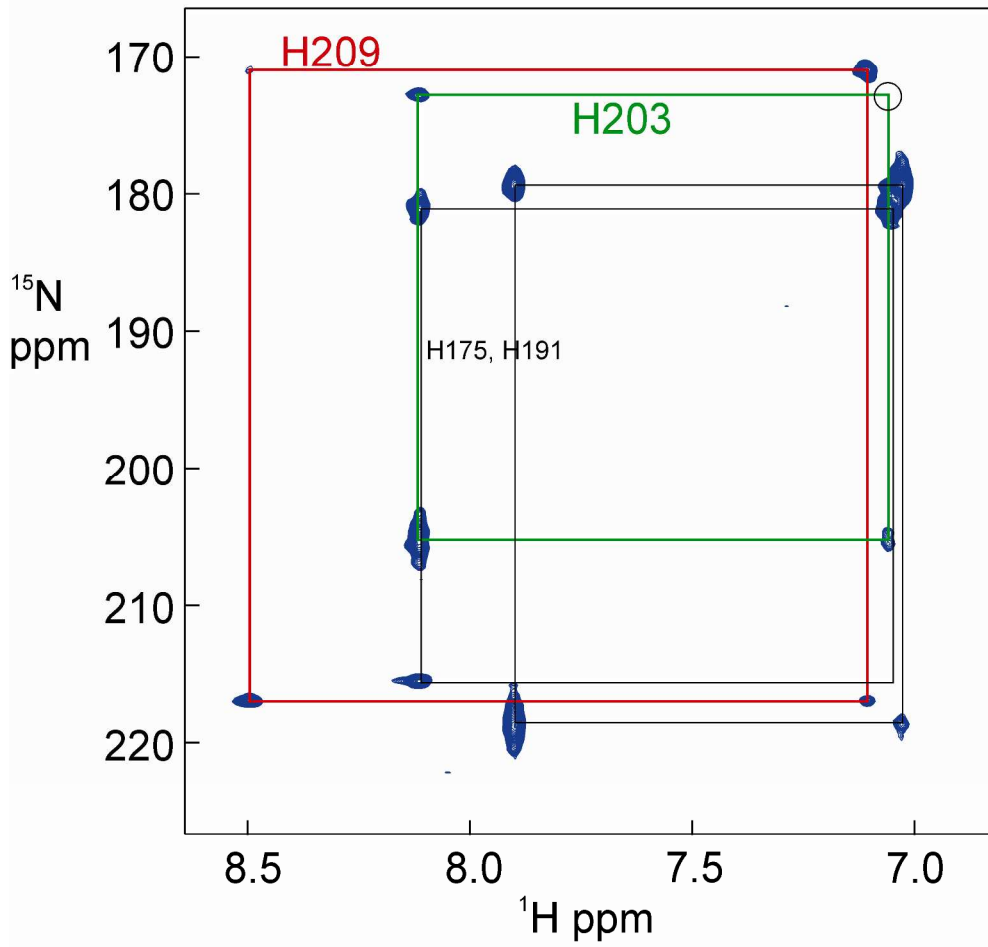
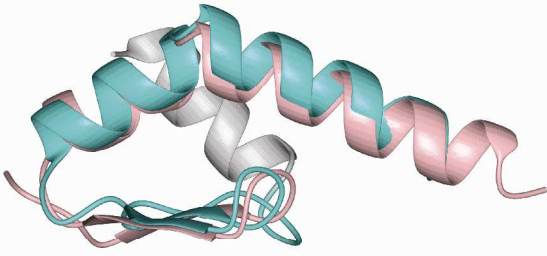


Figure S7

A



B

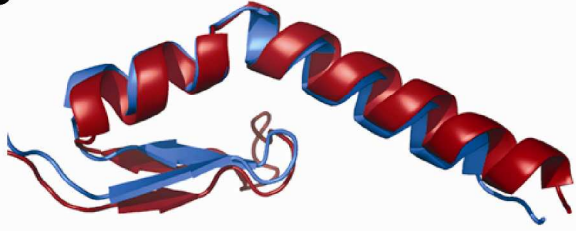


Figure S8